

# Infrared radiative forcing and atmospheric lifetimes of trace species based on observations from UARS

K. Minschwaner and R. W. Carver<sup>1</sup>

Department of Physics, New Mexico Institute of Mining and Technology, Socorro

B. P. Briegleb

National Center for Atmospheric Research, Boulder, Colorado

A. E. Roche

Lockheed Palo Alto Research Laboratory, Pal Alto, California

**Abstract.** Observations from instruments on the Upper Atmosphere Research Satellite (UARS) have been used to constrain calculations of infrared radiative forcing by CH<sub>4</sub>, CCl<sub>2</sub>F<sub>2</sub>, and N<sub>2</sub>O and to determine lifetimes of CCl<sub>2</sub>F<sub>2</sub> and N<sub>2</sub>O. Radiative forcing is calculated as a change in net infrared flux at the tropopause that results from an increase in trace gas amount from preindustrial (1750) to contemporary (1992) times. Latitudinal and seasonal variations are considered explicitly, using distributions of trace gases and temperature in the stratosphere from UARS measurements and seasonally averaged cloud statistics from the International Satellite Cloud Climatology Project. Top-of-atmosphere fluxes calculated for the contemporary period are in good agreement with satellite measurements from the Earth Radiation Budget Experiment. Globally averaged values of the radiative forcing are 0.550, 0.132, and 0.111 W m<sup>-2</sup> for CH<sub>4</sub>, CCl<sub>2</sub>F<sub>2</sub>, and N<sub>2</sub>O, respectively. The largest forcing occurs near subtropical latitudes during summer, predominantly as a result of the combination of cloud-free skies and a high, cold tropopause. Clouds are found to play a significant role in regulating infrared forcing, reducing the magnitude of the forcing by 30–40% compared with the case of clear skies. The vertical profile of CCl<sub>2</sub>F<sub>2</sub> is important in determining its radiative forcing; use of a height-independent mixing ratio in the stratosphere leads to an overprediction of the forcing by 10%. The impact of stratospheric profiles on radiative forcing by CH<sub>4</sub> and N<sub>2</sub>O is 2% or less. UARS-based distributions of CCl<sub>2</sub>F<sub>2</sub> and N<sub>2</sub>O are used also to determine global destruction rates and instantaneous lifetimes of these gases. Rates of photolytic destruction in the stratosphere are calculated using solar ultraviolet irradiances measured on UARS and a line-by-line model of absorption in the oxygen Schumann-Runge bands. Lifetimes are 114 ± 22 and 118 ± 25 years for CCl<sub>2</sub>F<sub>2</sub> and N<sub>2</sub>O, respectively.

## 1. Introduction

Increases in the atmospheric abundances of CH<sub>4</sub>, CCl<sub>2</sub>F<sub>2</sub> (CFC-12) and N<sub>2</sub>O from the preindustrial to the present time have had a significant effect on the radiative and photochemical state of the atmosphere.

<sup>1</sup>Now at School of Meteorology, University of Oklahoma, Norman.

The enhanced infrared opacity as a result of these changes accounts for nearly one third of the postindustrial, greenhouse gas direct radiative forcing [*Intergovernmental Panel on Climate Change (IPCC)*, 1995]. In addition, CH<sub>4</sub>, CCl<sub>2</sub>F<sub>2</sub>, and N<sub>2</sub>O are significant sources of hydrogen, chlorine, and nitrogen radicals in the stratosphere and thus play an important role in the budget of stratospheric ozone. Global destruction rates of CCl<sub>2</sub>F<sub>2</sub> and N<sub>2</sub>O are determined primarily by ultraviolet photolysis in the stratosphere.

Although the longwave effects of trace gas increases were recognized some time ago [*Ramanathan*, 1975; *Wang et al.*, 1976], it is only recently that global distributions have become available for including latitudinal

Copyright 1998 by the American Geophysical Union.

Paper number 98JD02116.  
0148-0227/98/98JD-02116\$09.00

as well as seasonal effects. Calculations of radiative forcing, for the most part, have been based on results using global mean vertical profiles of temperature, water vapor, and ozone [Wang *et al.*, 1980; Hansen *et al.*, 1981; Ramanathan *et al.*, 1987]. The computed flux, however, may not be identical to the global average of separate calculations at each latitude [see, for example, World Meteorological Organization (WMO), Chapter 7 1991; Pinnock *et al.*, 1995; Myhre and Stordal, 1997; Freckleton *et al.*, 1998]. Furthermore, the decrease in concentrations of CH<sub>4</sub>, CCl<sub>2</sub>F<sub>2</sub>, and N<sub>2</sub>O with increasing altitude above the tropopause can influence the downward flux at the tropopause level, thereby impacting the radiative forcing [Ramanathan *et al.*, 1985]. These effects are accounted for implicitly within the context of two- and three-dimensional model studies [Kiehl and Briegleb, 1993; Hauglustaine *et al.*, 1994; Hansen *et al.*, 1997], with trace gas distributions determined internally by the model.

The importance of CH<sub>4</sub>, N<sub>2</sub>O, and most CFCs to the Earth's longwave radiation budget is due largely to the spectral location of the principal IR bands involved. Most are located within, or near, a relatively transparent spectral window between 8 and 12  $\mu$ m. The accurate specification of stratospheric ozone in the radiative calculations is thus important due to the presence of the O<sub>3</sub> 9.6- $\mu$ m band. Equally important, tropospheric clouds are strong sources of opacity in the 8 to 12- $\mu$ m window, and the proper representation of clouds is critical to the evaluation of radiative forcing at the tropopause. High clouds in the troposphere have been shown to influence strongly the stratospheric IR heating by ozone [e.g., Dessler *et al.*, 1996], as well as the radiative forcing by tropospheric O<sub>3</sub> [Forster *et al.*, 1996] and CFC replacements [Pinnock *et al.*, 1995].

The destruction of N<sub>2</sub>O and CCl<sub>2</sub>F<sub>2</sub> is thought to take place primarily in the stratosphere. Most of the loss occurs through photodissociation by absorption of solar ultraviolet radiation in the 190- to 220-nm spectral region, at altitudes between 20 and 40 km [Minschwaner *et al.*, 1993]. Lifetimes for N<sub>2</sub>O and CFC compounds have been estimated using two-dimensional photochemical models of the middle atmosphere [e.g., Ko and Sze, 1982], with calculated values determined by the balance between stratospheric loss and influx to the stratosphere by cross-tropopause transport in the tropics. A more empirical method applies calculated destruction rates to observed distributions in the stratosphere [Johnston *et al.*, 1979]. If the source terms are accurately known, then the lifetime can also be estimated from the total atmospheric burden [e.g., Kaye *et al.*, 1994]. A novel technique outlined by Plumb and Ko [1992] employs correlations between long-lived tracers in the stratosphere to determine lifetime ratios. The use of this technique is discussed within the framework of three-dimensional model calculations by Avallone and Prather [1997] and is applied to ER-2 observations in the stratosphere by Volk *et al.* [1997].

The present study is motivated by the availability of global-scale observations from the Upper Atmosphere Research Satellite (UARS), which are relevant to the

evaluation of radiative forcings and lifetimes of trace gases. UARS measurements of CH<sub>4</sub>, CCl<sub>2</sub>F<sub>2</sub>, N<sub>2</sub>O, O<sub>3</sub>, H<sub>2</sub>O, temperature, and solar ultraviolet irradiances are used to represent the physical and chemical state of the contemporary stratosphere. Complementary measurements of trace gas mixing ratios at the surface, mean cloud statistics from the International Satellite Cloud Climatology Project (ISCCP), and average longwave fluxes from the Earth Radiation Budget Experiment (ERBE) are used to complete this picture. The goal is to take advantage of the unprecedented spatial and temporal coverage of UARS measurements and apply them to the evaluation of radiative forcing by CH<sub>4</sub>, CCl<sub>2</sub>F<sub>2</sub>, and N<sub>2</sub>O and to determine atmospheric lifetimes for CCl<sub>2</sub>F<sub>2</sub> and N<sub>2</sub>O.

## 2. UARS Distributions of Trace Gases and Temperature

Climatological distributions of trace gases were constructed from zonal averages of UARS observations over 2-month periods bracketing the equinoxes and solstices. The total time interval extends from March 1992 to January 1993. All calculations were carried out on a 5° latitude grid from 77.5°S to 77.5°N. Constant values were used poleward of 77.5° for the purposes of obtaining global averages. Vertical levels were spaced 100 mbar apart in the troposphere, decreasing to 10-20 mbar near the tropopause and lower stratosphere. Vertical resolution in the middle and upper stratosphere was approximately 3 km.

Distributions of CH<sub>4</sub>, CCl<sub>2</sub>F<sub>2</sub>, and N<sub>2</sub>O in the stratosphere were derived from vertical profiles measured by the Cryogen Limb Array Etalon Spectrometer (CLAES) on board UARS. The CLAES instrument observed limb emission in vibration-rotation spectra between 3.5 and 13  $\mu$ m for retrieval of trace gas mixing ratios, pressure, and temperature [Roche *et al.*, 1993]. Version 7, level 3AT data were used for all three gases. Averages for each latitude bin were obtained by weighting all values according to the data quality indicator associated with each point. The zonally averaged vertical profile was linearly interpolated from the UARS standard pressure levels to our adopted vertical grid. CLAES data were used from 0.1 mbar down to 46 mbar; values below this level were determined using a cubic spline interpolation to the tropopause (specification of the tropopause pressure is discussed below).

Mixing ratios in the troposphere, assumed to be height independent due to mixing, were obtained from 1991-1992 measurements from the surface network operated by the Climate Monitoring and Diagnostics Laboratory for CH<sub>4</sub> [Tans *et al.*, 1992] and for CCl<sub>2</sub>F<sub>2</sub> and N<sub>2</sub>O [Montzka *et al.*, 1992]. We approximated latitudinal gradients in mixing ratios using linear fits to data from six surface stations ranging from 82.5°N to 40.7°S. This variation is small for N<sub>2</sub>O (less than 1% from pole to pole) but is significant for CH<sub>4</sub> (~9% pole to pole) and CCl<sub>2</sub>F<sub>2</sub> (~6%).

Other model inputs which are constrained by data from UARS include stratospheric O<sub>3</sub> and H<sub>2</sub>O. Cor-

rect specification of ozone is of some importance for the infrared flux due to spectral overlaps in the wings of the O<sub>3</sub> 9.6- $\mu$ m band and the N<sub>2</sub>O 7.8- $\mu$ m band, the CH<sub>4</sub> 7.7- $\mu$ m band, and CCl<sub>2</sub>F<sub>2</sub> absorption bands near 9  $\mu$ m. The 6.7- $\mu$ m band of water has an effect also on the N<sub>2</sub>O and CH<sub>4</sub> bands. In the ultraviolet, the short-wavelength tail of the ozone Hartley band contributes significantly to the opacity near 200 nm and therefore impacts photodissociation of both CCl<sub>2</sub>F<sub>2</sub> and N<sub>2</sub>O. Zonally averaged distributions of O<sub>3</sub> and H<sub>2</sub>O were compiled based on measurements from the UARS Microwave Limb Sounder (MLS), which observes limb emission at millimeter wavelengths [Waters 1993; Froidevaux et al., 1994]. Version 3, level 3AT data from the 205-GHz radiometer were used for O<sub>3</sub>; data from the 183-GHz radiometer were used for H<sub>2</sub>O. Zonal and seasonal averages of MLS measurements above 50 mbar were constructed in a manner similar to the CLAES data described above. Ozone in the troposphere was based on climatological values from Oltmans [1981] and Levy et al. [1985]. Tropospheric water vapor was specified on the basis of standard Air Force Geophysics Laboratory (AFGL) models [Anderson et al., 1986] with values interpolated in season and latitude.

The vertical profile of temperature is another important parameter in the calculation of infrared forcing. Temperatures in the upper atmosphere have an impact also on ultraviolet photolysis through the temperature dependence of absorption cross sections, most notably in the O<sub>2</sub> Schumann-Runge (S-R) bands, with a corresponding effect on the penetration of ultraviolet radiation to the middle and lower stratosphere. Temperatures were adopted from the National Meteorological Center (NMC) analysis [McPherson et al., 1979], which are included as correlative data in the UARS data distribution. NMC temperatures were averaged over season and latitudes, similar to the CLAES trace gas data, from the surface to 70 mbar. CLAES measurements of temperature were used above 70 mbar. These agree well ( $\approx \pm 1$  K) with lidar and rocketsonde measurements of temperature up to the 1-mbar pressure level.

As discussed by Myhre and Stordal [1997] and Freckleton et al. [1998], specification of the tropopause pressure is a crucial aspect of determining the magnitude of radiative forcing. Owing to changes in tropopause pressure with latitude, adoption of a global-mean tropopause height can produce errors of up to 10% in the instantaneous, global-mean forcing [Myhre and Stordal, 1997]. In addition, Freckleton et al. [1998] showed that the choice of tropopause definition (i.e., lapse rate criteria, temperature minimum, top of convective level) can influence radiative forcing results by up to 9%. For the calculations presented below, we defined the tropopause height according to location of minima in temperature profiles at each latitude.

Distributions of CH<sub>4</sub>, CCl<sub>2</sub>F<sub>2</sub>, N<sub>2</sub>O, and O<sub>3</sub> for the September-October 1992 time period are shown in Figure 1. The dashed horizontal lines indicate the pressure level which divides UARS-based distributions from the region of interpolation. The tropopause pressure is shown by the bottom dashed curve in each panel. Of

particular importance for our calculations are the decreases in mixing ratios of CH<sub>4</sub>, CCl<sub>2</sub>F<sub>2</sub>, and N<sub>2</sub>O in the stratosphere as well as latitudinal variations in vertical profiles. Distributions of H<sub>2</sub>O and temperature for the same time period are shown in Figure 2, along with the distributions of cloud fraction and heights assumed in the calculations. These are derived from averages over the 1983-1990 time period for low, middle, and high cloud fractions from the International Satellite Cloud Climatology Project (ISCCP) [Rossow and Schiffer, 1991]. Low clouds are assumed to be located between 850 and 750 mbar, independent of latitude. Middle-level clouds are placed in a 100-mbar-thick layer centered near 500 mbar at middle and high latitudes, and near 550 mbar in tropics, as shown in Figure 2. High clouds are located in a 20-mbar-thick layer located just below the tropopause.

### 3. Radiative Calculations

As discussed by IPCC [1995], the concept of radiative forcing is a valuable measure of the first-order climatic impact of a greenhouse gas. The forcing is defined by the change in net infrared flux at the tropopause due to a prescribed change in greenhouse gas amount, holding all other model parameters fixed (except for stratospheric temperatures, as discussed below). Adoption of the tropopause as a reference is motivated by the fact that a change in radiative flux at this level appropriately expresses the radiative forcing of the climate system as a whole, since the surface and troposphere are a tightly coupled thermodynamic system. In addition, defining the forcing in terms of the radiative flux change avoids uncertainties associated with a given climate response, for example, surface temperature, which depends on sensitivities and feedbacks that are evidently model-dependent [e.g., IPCC, 1990]. However, care must be taken to account for the temperature response in the stratosphere [Hansen et al., 1981; Ramanathan et al., 1987]. By maintaining radiative equilibrium (or constant heating/cooling) in the stratosphere, any change in flux at the tropopause is then the same as at the top of the atmosphere (TOA).

Infrared fluxes were calculated using a longwave-band model developed at the National Center for Atmospheric Research. This is a 100-cm<sup>-1</sup> band model which includes infrared opacity by H<sub>2</sub>O, CO<sub>2</sub>, and O<sub>3</sub>, and considers also the major absorption bands of CH<sub>4</sub>, N<sub>2</sub>O, CFC-11, and CFC-12. The code is similar in many respects to the Community Climate Model, Version 2 (CCM2) radiation code described by Briegleb [1992]. Line parameters for H<sub>2</sub>O, CO<sub>2</sub>, O<sub>3</sub>, CH<sub>4</sub>, and N<sub>2</sub>O are based on the HITRAN database [Rothman, 1986]. Absorption cross sections for CFC-11 and CFC-12, averaged over the 100 cm<sup>-1</sup> bands, are from Massie et al. [1991]. For the trace gases of interest here, the important longwave bands considered include the 7.7- $\mu$ m band of CH<sub>4</sub>, the 4.5-, 7.8-, and 17- $\mu$ m bands of N<sub>2</sub>O (see Figure 2 of Briegleb [1992]), and the 8.7-, 9.1-, and 10.9- $\mu$ m bands of CCl<sub>2</sub>F<sub>2</sub>.

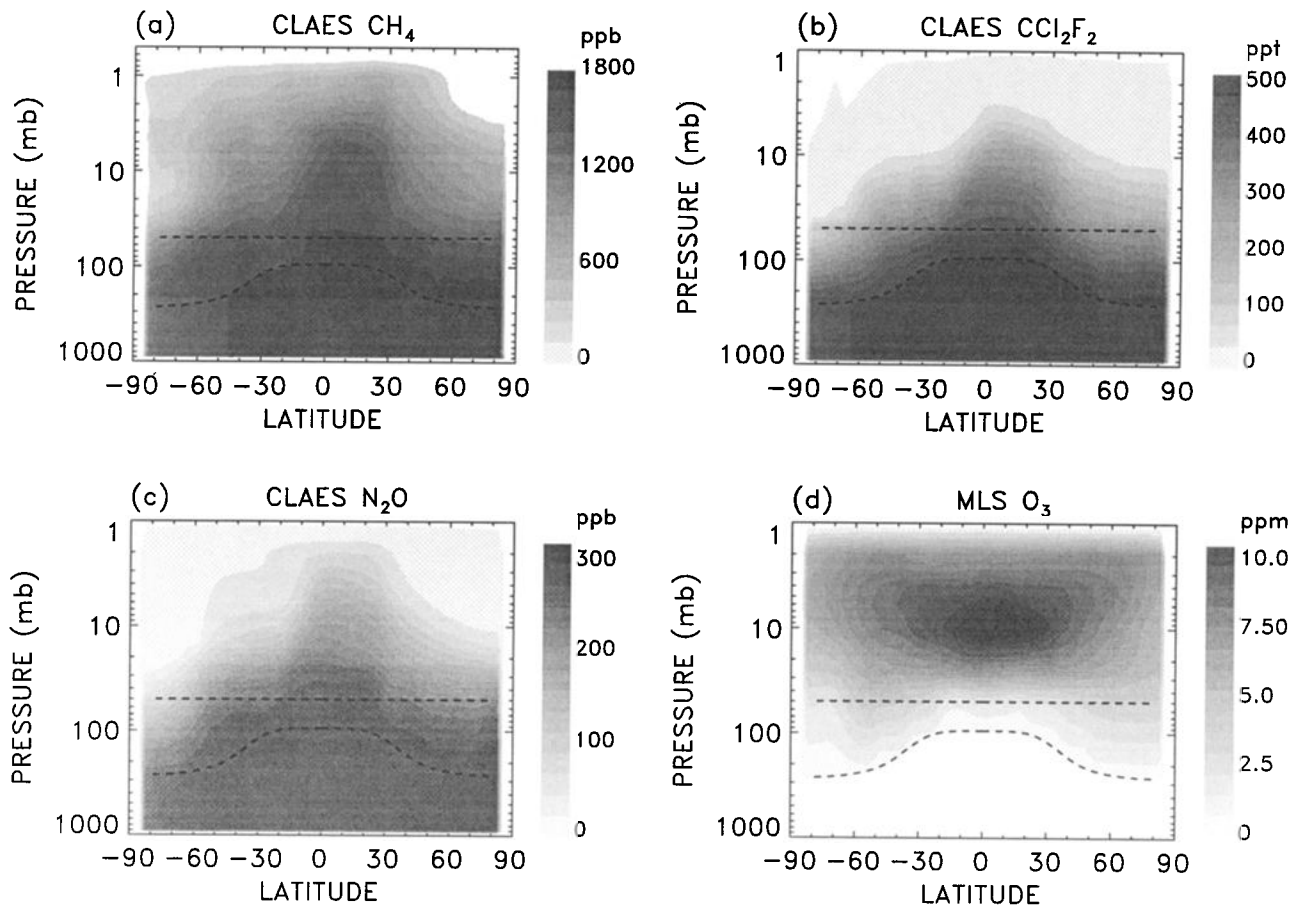


**Figure 1.** Distributions of (a)  $\text{CH}_4$  (in ppb), (b)  $\text{CCl}_2\text{F}_2$  (in ppt), (c)  $\text{N}_2\text{O}$  (in ppb), and (d)  $\text{O}_3$  (in ppm) used in the radiative calculations for the September-October contemporary period. Dashed curves indicate the tropopause and the lowest pressure level for UARS data. Tropospheric mixing ratios are specified as described in the text.

Net longwave fluxes calculated with this model agree with line-by-line calculations to within 1% [Briegleb, 1992]. We have, in addition, compared results for flux changes induced by changes in  $\text{CH}_4$  and  $\text{N}_2\text{O}$  with line-by-line calculations by Clough and Iacono [1995]. Results at the tropopause agree to within 10%. Figure 3 compares the TOA flux calculated with the model with measurements from the Earth Radiation Budget Experiment (ERBE) [Barkstrom, 1984] averaged over the 1985-1988 period. The agreement is within the uncertainties in flux ( $\pm 5 \text{ W m}^{-2}$ ) for nearly all latitudes and seasons. Comparison of model shortwave albedo with ERBE averages (not shown) also indicate a good level of agreement.

Results for June-July (Figure 3a) clearly show the impact of high clouds near the Intertropical Convergence Zone between  $5^\circ$  and  $10^\circ\text{N}$  which give rise to a minimum in TOA flux. This minimum shifts to south of the equator in both the ERBE observations and model calculations for December-January (Figure 3b). Calculated TOA fluxes are sensitive to assumptions of cloud liquid water paths (lwp) and effective drop radii ( $r_e$ ) assumed in the model. We adopted values for the three cloud types that are consistent with measurements [Stephens,

1978; Stephens and Platt, 1987]; these are identical to the values used by Dessler *et al.* [1996] (lwp = 125, 75, 15  $\text{g m}^{-2}$ , and  $r_e = 10, 11, 18 \mu\text{m}$ , for low, middle, and high clouds, respectively). Surface emissivity was fixed at 0.92, independent of latitude and season. This value represents an estimate of the weighted mean of sea surface ( $e \approx 0.92-0.96$ ), sand (0.85-0.90), and snow (0.85-0.99). Calculated forcings were found to be relatively insensitive to the precise choice of surface longwave emissivity.

For the determination of instantaneous lifetimes, photochemical loss due to ultraviolet photodissociation was calculated using the high-resolution radiation code described by Minschwaner *et al.* [1993]. Solar irradiances above the atmosphere were specified according to measurements from the Solar Stellar Irradiance Comparison Experiment (SOLSTICE) on board UARS, averaged over the month of March 1992. These are high-resolution (0.1 nm) measurements of the full-disk, solar spectral irradiance between 115 and 420 nm [Rottman *et al.*, 1993]. Calibration is maintained to within 1% using a collection of bright blue stars as radiance standards [Woods *et al.*, 1993]. Version 7, level 3BS irradiances with a spectral resolution of 1 nm were used

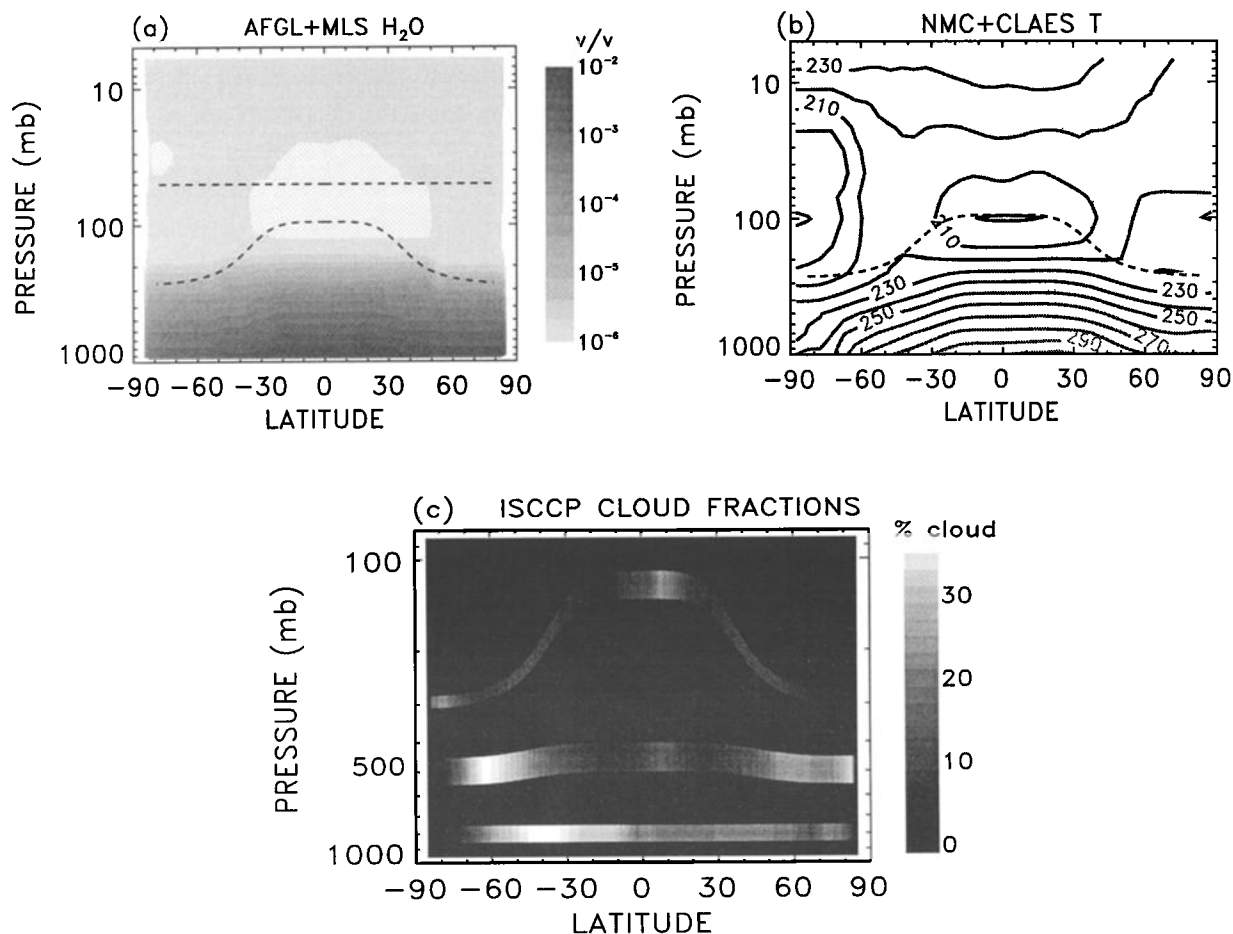


**Figure 2.** Distributions of (a) H<sub>2</sub>O (volume mixing ratio), (b) temperature (degrees Kelvin), and (c) cloud fractions (percent) used in the radiative calculations for the September-October preindustrial and contemporary time periods.

over the full spectral range. Oxygen cross sections in the S-R band region followed the line-by-line analysis by Minschwaner *et al.* [1992]. Cross sections for the O<sub>2</sub> Herzberg continuum were adopted from Yoshino *et al.* [1988], and cross sections for O<sub>3</sub>, CCl<sub>2</sub>F<sub>2</sub>, and N<sub>2</sub>O were adopted from DeMore *et al.* [1994]. Below 205 nm, solar irradiances and all cross sections other than O<sub>2</sub> were linearly interpolated to the high-resolution (0.002 nm) spectral grid necessary to capture the rotational structure in O<sub>2</sub> S-R band absorption. Effects of scattering above 190 nm were included based on the formulation of Meier *et al.* [1982].

The instantaneous lifetime for each gas was determined from the ratio of its 1992 global inventory  $M$  by the calculated global removal rate  $L$ :

$$\tau(1992) = M/L \quad (1)$$

The two quantities in the above equations are defined by

$$M = 2\pi R_E^2 \int dz \int n(\phi, z, 1992) \cos \phi d\phi \quad (2)$$

$$L = 2\pi R_E^2 \int dt \int dz \int n(\phi, z, t) J(\phi, z, t) \cos \phi d\phi \quad (3)$$

where  $n(\phi, z, t)$  is the local concentration at latitude  $\phi$ , altitude  $z$ , and time  $t$  and where  $R_E$  is the Earth's radius. The corresponding loss frequency  $J$  is set primarily by photodissociation, although total loss includes a small contribution (5-10%) due to reaction with O(<sup>1</sup>D). Global fields of O(<sup>1</sup>D) were calculated based on a steady state between production due to photolysis of ozone, using the MLS ozone fields described above, and loss due to quenching by N<sub>2</sub> and O<sub>2</sub>. Rates for quenching and for reactions of O(<sup>1</sup>D) with CCl<sub>2</sub>F<sub>2</sub> and N<sub>2</sub>O followed recommended values by DeMore *et al.* [1994].

## 4. Results

### 4.1. Radiative Forcing

The radiative forcing from preindustrial (1750) to the 1992 time period was calculated using preindustrial mixing ratios of 700 ppb CH<sub>4</sub>, 0 ppt CCl<sub>2</sub>F<sub>2</sub>, and 275 ppb N<sub>2</sub>O in the troposphere [IPCC, 1995]. Except for CCl<sub>2</sub>F<sub>2</sub>, there are no corresponding estimates for stratospheric distributions. A reasonable approximation, however, is to assume the same relative distribu-

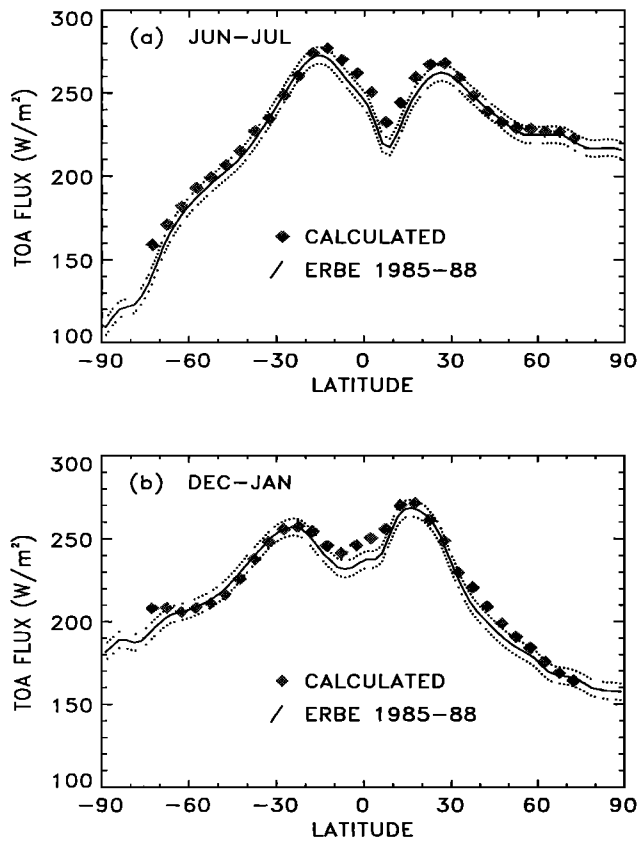


**Figure 3.** Top of atmosphere infrared fluxes for (a) June–July and (b) December–January. Diamonds indicate values calculated using the radiative model initialized with temperature, trace gas distributions, and clouds as described in the text. Solid curves represent averages of 1985–1988 observations from the Earth Radiation Budget Experiment.

tion as is currently observed. This follows from the fact that the stratospheric loss scales linearly with trace gas amount. Therefore preindustrial trace gas distributions were estimated by scaling all vertical profiles according to the ratio of preindustrial to present-day mixing ratios in the troposphere. It should be noted that the radiative forcing for each gas was computed by using the observed change in abundance of that gas alone, with all other trace gases held fixed at their preindustrial amounts.

The model was modified for the study of radiative forcing by allowing stratospheric temperatures to adjust so that stratospheric heating/cooling rates were identical to values calculated for the preindustrial stratosphere. This approach essentially assumes a fixed dynamical heating/cooling in the stratosphere rather than complete radiative equilibrium, but the final results should be comparable [Ramanathan and Dickinson, 1979]. Temperatures were adjusted iteratively until the net heating rate changed by less than  $5 \times 10^{-4}$  K day<sup>-1</sup> at all levels above the tropopause.

The magnitude of radiative forcing for CH<sub>4</sub>, CCl<sub>2</sub>F<sub>2</sub>, and N<sub>2</sub>O as a function of season and latitude is shown

in Plate 1. Values are largest in the summer subtropics, consistent with a relatively warm surface, cold tropopause, and comparatively clear skies. A similar behavior was noted in the three-dimensional simulations by Kiehl and Briegleb [1993]. Latitudinal values of the forcing vary by up to a factor of 3 between the tropics and high latitudes in the winter hemisphere. Also included in Plate 1 is the assumed distribution of high cloud as a function of season and latitude. The patterns indicate a high degree of anticorrelation between high cloud fraction and the magnitude of radiative forcing for all three gases. These results are consistent with variations with respect to latitude (primarily vertical profiles of temperature) and cloud cover found for hydrofluorocarbon radiative forcings by Pinnock *et al.* [1995] and for SF<sub>6</sub> and CO<sub>2</sub> forcings calculated by Myhre and Stordal [1997].

Globally averaged values of radiative forcing are listed in Table 1, along with results from the 42°N summer calculation and values reported by IPCC [1995]. The digit representing mW m<sup>-2</sup> should be interpreted with caution in light of the uncertainties in spectroscopic and atmospheric input parameters. Values shown in Table 1 imply that the use of a midlatitude summer atmosphere to represent the global average leads to an overprediction of between 4 and 8% in the radiative forcing. Differences between the UARS-based forcings and IPCC [1995] values are +17%, -6%, and -21% for CH<sub>4</sub>, CCl<sub>2</sub>F<sub>2</sub>, and N<sub>2</sub>O, respectively. The discrepancy for CCl<sub>2</sub>F<sub>2</sub> is within the uncertainty (15%) associated with IPCC [1995] forcing estimates but slightly outside this bound for CH<sub>4</sub>. It has been noted, however, that other studies have in fact indicated higher values (up to 20%) for the radiative forcing of CH<sub>4</sub> [IPCC, 1995], which is consistent with results presented here.

The reason for the large difference with IPCC [1995] in the computed N<sub>2</sub>O forcing is unclear. The treatment of clouds may play a role; the clear-sky N<sub>2</sub>O forcing at midlatitudes increases to 0.146 W m<sup>-2</sup> (see below). However, a systematic difference in cloud fractions or radiative properties would be expected to have the same sign for all three gases. Use of a midlatitude summer atmosphere with clouds only partially improves the agreement. The strong spectral overlap between CH<sub>4</sub> and N<sub>2</sub>O may also be a factor in the discrepancy between N<sub>2</sub>O forcings. Results presented here explicitly include the spectral overlap using a fixed abundance of 700 ppb CH<sub>4</sub>. The N<sub>2</sub>O forcing from IPCC [1995] is calculated based on an analytic fit to model calculations that includes an empirically determined correction for the spectral overlap.

Sensitivities of calculated forcing clouds and to vertical profiles of mixing ratio in the stratosphere are summarized in Table 2. As expected, forcings are larger for clear skies because absorbing gases at the tropopause and in the lower stratosphere see a warmer effective temperature below, leading to an enhanced greenhouse influence. Differences range between 28 and 36% at midlatitudes and are even more pronounced in tropics. The latter result arises due to the higher contrast in

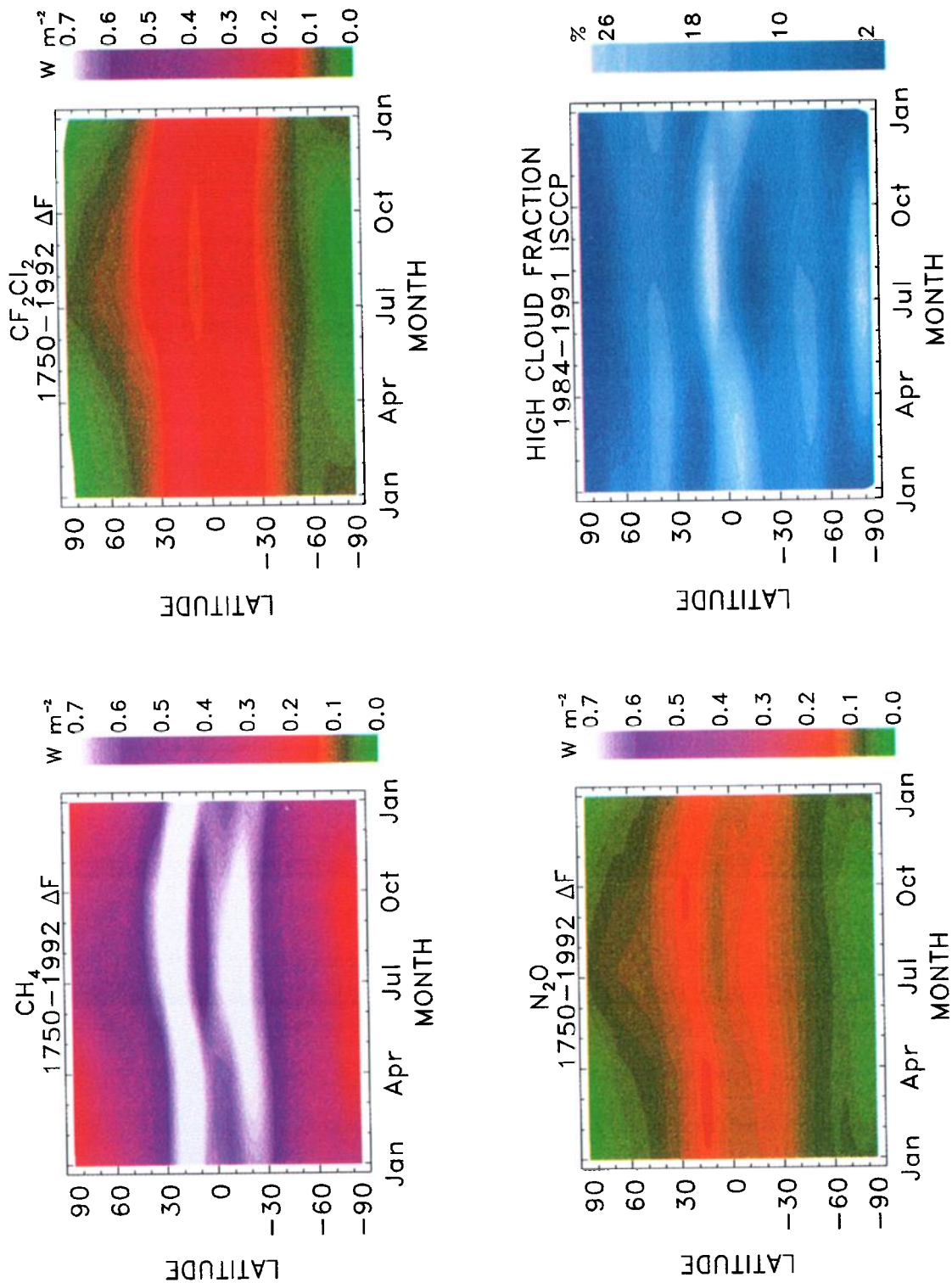


**Plate 1.** Seasonal and latitudinal dependence of the postindustrial radiative forcing calculated for  $CH_4$  (upper left), (b)  $CF_2Cl_2$  (upper right), and  $N_2O$  (lower left). All forcings are in  $W m^{-2}$ . Also shown (lower right) is the distribution of high cloud fraction used in the calculations.

**Table 1.** Trace Gas Radiative Forcing

Species	Global Average	42°N Summer	IPCC [1995]
CH <sub>4</sub>	0.550	0.579	0.47
CCl <sub>2</sub> F <sub>2</sub>	0.132	0.143	0.14
N <sub>2</sub> O	0.111	0.115	0.14

Values are in  $W m^{-2}$ .

temperature between cloud top and the lower troposphere in the tropics as compared with midlatitudes. Cloud effects are similar to the 36% clear-sky enhancement for CCl<sub>3</sub>F forcing at midlatitudes presented by Pinnock *et al.* [1995].

The impact of using realistic stratospheric profiles was discussed by Ramanathan *et al.* [1985] for CH<sub>4</sub> and N<sub>2</sub>O and more recently by Hansen *et al.* [1997] and Christidis *et al.* [1997] for CFCs and HCFCs. However, previous studies either assumed exponential decreases using a constant scale height or used model-calculated profiles instead of observed distributions. Our calculations show a negligible impact on CH<sub>4</sub> and N<sub>2</sub>O (Table 2), which is consistent with the results of Ramanathan *et al.* [1985]. The net IR flux at the tropopause does show a significant difference between the case of a uniform mixing ratio and one that decreases with height in the lower stratosphere. However, with the scaling procedures used here to approximate CH<sub>4</sub> and N<sub>2</sub>O mixing ratios in the preindustrial stratosphere, this flux difference appears in both the preindustrial and contemporary cases, and very nearly cancels out in the radiative forcing.

On the other hand, the forcing for CCl<sub>2</sub>F<sub>2</sub> is increased by up to 10% if a uniform mixing ratio is used to represent the contemporary atmosphere. One reason that this effect is larger than for CH<sub>4</sub> or N<sub>2</sub>O is that the preindustrial atmosphere contained no CCl<sub>2</sub>F<sub>2</sub>; therefore the difference in net flux between the case of a uniform and realistic vertical profile of CCl<sub>2</sub>F<sub>2</sub> translates directly to a difference in the computed radiative forcing. Furthermore, the opacity of the atmosphere is generally less for the CCl<sub>2</sub>F<sub>2</sub> bands (9–11  $\mu m$ ) in comparison with the major CH<sub>4</sub> (7.7  $\mu m$ ) and N<sub>2</sub>O (7.8  $\mu m$ ) absorption bands. Consequently, changes in CCl<sub>2</sub>F<sub>2</sub> abundances are felt over a greater range of altitudes, including the middle and upper stratosphere.

#### 4.2. Lifetimes for CCl<sub>2</sub>F<sub>2</sub> and N<sub>2</sub>O

Instantaneous lifetimes were calculated using the sum of global loss rates for the four separate seasons (equation (4)) and the mean atmospheric burden during the same period (equation (3)). Lifetimes for CCl<sub>2</sub>F<sub>2</sub> and N<sub>2</sub>O are  $114 \pm 22$  and  $118 \pm 25$  years, respectively. Uncertainties are estimated based on the standard deviation of the CLAES zonal means where loss rates are a maximum (12% for CCl<sub>2</sub>F<sub>2</sub> and 9% for N<sub>2</sub>O), uncertainty in actinic flux (5% in solar irradiance and 10% in

atmospheric transmission), and absorption cross section uncertainties (10% for CCl<sub>2</sub>F<sub>2</sub> and 15% for N<sub>2</sub>O).

Calculated rates for stratospheric loss were largest in the tropical midstratosphere. Globally integrated rates were found to be moderately dependent on season; removal rates were 12% larger during the equinoxes as compared with the solstices. These higher rates are a consequence of smaller solar zenith angles in the tropics during the equinoxes, with associated increases in actinic fluxes in the lower stratosphere.

Previous estimates of the CCl<sub>2</sub>F<sub>2</sub> lifetime range from 95 years [Ko *et al.*, 1991] to 180 years [Cunnold *et al.*, 1994]; the range for N<sub>2</sub>O is 110 years [Ko *et al.*, 1991] to 182 years [Golombek and Prinn, 1986]. Our results favor the lower end of these ranges and are in good agreement with previous instantaneous lifetimes, 116 years for CCl<sub>2</sub>F<sub>2</sub> and 123 years for N<sub>2</sub>O, obtained by Minschwaner *et al.* [1993]. The latter estimates were obtained using the same empirical technique and nearly identical calculations for photochemical loss as used here; however, the level of agreement is somewhat surprising in view of the fact that the trace gas distributions used by Minschwaner *et al.* [1993] were based on a relatively sparse collection of balloon and aircraft data.

The steady state lifetime, where emissions to the atmosphere exactly balance photochemical loss, is generally shorter than the instantaneous lifetime for gases whose concentrations are increasing with time. The difference arises from the time lag between temporal changes in abundances for the stratosphere relative to the troposphere. The distinction between steady state and instantaneous lifetime is small for N<sub>2</sub>O because the growth rate of about 0.25% year<sup>-1</sup> [Montzka *et al.*, 1992] does not significantly impact stratospheric/tropospheric abundances over timescales relevant for the turnover of stratospheric air (less than 5 years [Rosenlof and Holton, 1993]). However, the mean growth rate for CCl<sub>2</sub>F<sub>2</sub> is much larger, averaging about 3.5% year<sup>-1</sup> between 1988 and 1992 [Elkins *et al.*, 1993]. Assuming a mean age of between 2 and 4 years for midstratosphere air in the tropics [Hall and Plumb, 1994; Boering *et al.*, 1996] and an instantaneous lifetime of 114 years, the estimated steady state lifetime for CCl<sub>2</sub>F<sub>2</sub> is between 99 and 106 years. Including the uncertainty in instantaneous lifetimes yields steady state lifetimes of  $103 \pm 25$  years for CCl<sub>2</sub>F<sub>2</sub>, and  $117 \pm 26$  years for N<sub>2</sub>O.

**Table 2.** Forcing Sensitivities, Summer Season

Species	Clear Sky		Fixed Strat <sup>a</sup>	
	42°N	3°N	42°N	3°N
CH <sub>4</sub>	29	36	1	1
CCl <sub>2</sub> F <sub>2</sub>	36	51	8	10
N <sub>2</sub> O	28	35	2	1

Values are percent increases above standard cases.

<sup>a</sup>Constant trace gas mixing ratio above the tropopause.

Steady state lifetimes of 102 and 120 years for  $\text{CCl}_2\text{F}_2$  and  $\text{N}_2\text{O}$ , respectively, are presented by IPCC [1995]. These lifetimes, based primarily on results of 2-D model calculations, agree very well with our UARS-based values. Results from the Goddard Institute for Space Studies/UCI three-dimensional chemical transport model yield steady-state lifetimes of 90 and 113 years for  $\text{CCl}_2\text{F}_2$  and  $\text{N}_2\text{O}$ , respectively [Avallone and Prather, 1997], which are somewhat shorter than those calculated here but within the range of uncertainty. As noted by Avallone and Prather [1997], there may be a tendency in the model for excessive vertical mixing in the tropical stratosphere, leading to enhanced rates of calculated destruction. The use of observed tracer correlations by Volk *et al.* [1997] indicates lifetimes of 87 and 122 years for  $\text{CCl}_2\text{F}_2$  and  $\text{N}_2\text{O}$ , respectively. These are also consistent with our results, although the  $\text{CCl}_2\text{F}_2$  steady state lifetime is near the low range of the UARS-based value.

## 5. Conclusions

Our radiative calculations constrained by UARS and ISCCP observations imply a total postindustrial forcing of  $0.79 \text{ W m}^{-2}$  due to increasing burdens of trace gases  $\text{CH}_4$ ,  $\text{CCl}_2\text{F}_2$ , and  $\text{N}_2\text{O}$ . For comparison, the estimated  $\text{CO}_2$ -induced forcing is  $1.56 \text{ W m}^{-2}$  over the same period [IPCC, 1995]. Equally important, our results indicate a strong dependence of the trace gas forcing on season and latitude. At midlatitudes, forcings are largest during the summer-fall season, and seasonal amplitudes are about 10%. Latitudinal values of the trace gas forcing increase by nearly a factor of 3 between the winter high latitudes and subtropics.

Cloud effects, particularly the fraction of high clouds in the tropics, play a significant role in regulating the radiative forcing. Clouds reduce the clear-sky forcing by about 30% at midlatitudes and by up to 50% in the tropics. In this regard it is important to note that even small changes in cloud amount could be just as important as changes in trace gas abundances. In addition, the stratospheric distribution of  $\text{CCl}_2\text{F}_2$  is important in determining the magnitude of its forcing. Since the stratospheric profile of  $\text{CCl}_2\text{F}_2$  is determined in part by UV photolysis and opacity by  $\text{O}_3$ , this implies a possibly important connection between the photochemical and climatic influence of this gas.

The radiative forcing and atmospheric lifetime both enter into the evaluation of the global warming potential (GWP) of a greenhouse gas. The GWP is defined as the time-integrated radiative forcing from the instantaneous release of 1 kg of trace gas, expressed relative to that from 1 kg of  $\text{CO}_2$  [IPCC, 1990]. For the trace species considered here, the magnitudes of postindustrial radiative forcings and atmospheric lifetimes are broadly similar to currently accepted values, implying GWPs which are consistent with results presented by IPCC [1995]. However, our radiative forcing by  $\text{N}_2\text{O}$  is 21% smaller in magnitude, and our steady state lifetime is about 2% shorter; taken together, these results sug-

gests that the  $\text{N}_2\text{O}$  GWP may be about 23% less than the currently recommended value.

**Acknowledgments.** This research was supported by UARS guest investigator grant NAG 5-2847 from NASA's Mission to Planet Earth Program. The National Center for Atmospheric Research is sponsored by the National Science Foundation. We thank Guy Brasseur, David Edwards, and Keith Shine for useful comments and discussions and Michael Iacono for providing results of line-by-line radiative calculations. Helpful suggestions from two anonymous reviewers improved the manuscript very much and are appreciated. UARS data was obtained from the NASA GFSC Distributed Active Archive Center and from CD-ROMs made available by NASA GSFC.

## References

- Anderson, G. P., S. A. Clough, F. X. Kneizys, J. H. Chetwynd, and E. P. Shettle, AFGL atmospheric constituent profiles (0-120km), *AFGL Tech. Rep., AFGL-TR-86-0110*, 43 pp., Air Force Phillips Lab., Hansom Air Force Base, Mass., 1986.
- Avallone, L. M., and M. J. Prather, Tracer-tracer correlations: Three-dimensional model simulations and comparisons to observations, *J. Geophys. Res.*, **102**, 19,233-19,246, 1997.
- Barkstrom, B. R., The Earth Radiation Budget Experiment (ERBE), *Bull. Am. Meteorol. Soc.*, **65**, 1170-1185, 1984.
- Boering, K. A., S. C. Wofsy, B. C. Baube, H. R. Schneider, M. Loewenstein, J. R. Podolske, and T. J. Conway, Stratospheric mean ages and transport rates from observations of carbon dioxide and nitrous oxide, *Science*, **274**, 1340-1343, 1996.
- Briegleb, B. P., Longwave band model for thermal radiation in climate studies, *J. Geophys. Res.*, **97**, 11,475-11,485, 1992.
- Christidis, N., M. D. Hurley, S. Pinnock, K. P. Shine, and T. J. Wallington, Radiative forcing of climate change by CFC-11 and possible CFC replacements, *J. Geophys. Res.*, **102**, 19,597-19,609, 1997.
- Clough, S. A., and M. J. Iacono, Line-by-line calculation of atmospheric fluxes and cooling rates, 2, Application to carbon dioxide, ozone, methane, nitrous oxide and the halocarbons, *J. Geophys. Res.*, **100**, 16,519-16,535, 1995.
- Cunnold, D. M., P. J. Fraser, R. F. Weiss, R. G. Prinn, P. G. Simmonds, B. R. Miller, F. N. Alyea, and A. J. Crawford, Global trends and annual releases of  $\text{CFCl}_3$  and  $\text{CF}_2\text{Cl}_2$  estimated from ALE/GAGE and other measurements from July 1978 to June 1991, *J. Geophys. Res.*, **99**, 1107-1126, 1994.
- DeMore, W. B., S. P. Sander, D. M. Golden, R. F. Hampson, M. J. Kurylo, C. J. Howard, A. R. Ravishankara, C. E. Kolb, and M. J. Molina, Chemical kinetics and photochemical data for use in stratospheric modeling, Evaluation 11, *JPL Pub. 94-26*, Jet Propul. Lab., Pasadena, Calif., 1994.
- Dessler, A. E., K. Minschwaner, E. M. Weinstock, E. J. Hints, J. G. Anderson, and J. M. Russell III, The effects of tropical cirrus clouds on the abundance of lower stratospheric ozone, *J. Atmos. Chem.*, **23**, 209-220, 1996.
- Elkins, J. W., T. M. Thompson, T. H. Swanson, J. H. Butler, B. D. Hall, S. O. Cummings, D. A. Fisher, and A. G. Raffo, Decrease in the growth rates of atmospheric chlorofluorocarbons 11 and 12, *Nature*, **364**, 780-783, 1993.
- Forster, P. M. de F., C. E. Johnson, K. S. Law, J. A. Pyle, and K. P. Shine, Further estimates of radiative forcing due to tropospheric ozone changes, *Geophys. Res. Lett.*, **23**, 3321-3324, 1996.

- Freckleton, R. S., E. J. Highwood, K. P. Shine, O. Wild, K. S. Law, and M. G. Sanderson, Greenhouse gas radiative forcing: Averaging and inhomogeneities in trace gas distribution, *Q. J. R. Meteorol. Soc.*, in press, 1998.
- Froidevaux, L., J. W. Waters, W. G. Read, L. S. Elson, D. A. Flower, and R. F. Jarnot, Global ozone observations from the UARS MLS: An overview of zonal-mean results, *J. Atmos. Sci.*, *51*, 2846-2866, 1994.
- Golombek, A., and R. G. Prinn, A global three-dimensional model of the circulation and chemistry of  $\text{CFCl}_3$ ,  $\text{CF}_2\text{Cl}_2$ ,  $\text{CH}_3\text{CCl}_3$ ,  $\text{CCl}_4$ , and  $\text{N}_2\text{O}$ , *J. Geophys. Res.*, *91*, 3985-4001, 1986.
- Hall, T. M., and R. A. Plumb, Age as a diagnostic of stratospheric transport, *J. Geophys. Res.*, *99*, 1059-1070, 1994.
- Hansen, J., D. Johnson, A. Lacis, S. Lebedeff, P. Lee, D. Rind, and G. Russell, Climate impact of increasing atmospheric carbon dioxide, *Science*, *213*, 957-966, 1981.
- Hansen, J., M. Sato, and R. Ruedy, Radiative forcing and climate response, *J. Geophys. Res.*, *102*, 6831-6864, 1997.
- Hauglustaine, D. A., C. Granier, G. P. Brasseur, and G. Megie, The importance of atmospheric chemistry in the calculation of radiative forcing on the climate system, *J. Geophys. Res.*, *99*, 1173-1186, 1994.
- Intergovernmental Panel on Climate Change, *Climate Change: The IPCC Scientific Assessment*, edited by J. T. Houghton, C. J. Jenkins, and J. J. Ephraums, 365 pp., Cambridge Univ. Press, New York, 1990.
- Intergovernmental Panel on Climate Change, *Climate Change 1994, Radiative Forcing of Climate Change and An Evaluation of the IPCC IS92 Emission Scenarios*, 339 pp., Cambridge Univ. Press, New York, 1995.
- Johnston, H. S., O. Serang, and J. Podolske, Instantaneous global nitrous oxide photochemical rates, *J. Geophys. Res.*, *84*, 5077-5082, 1979.
- Kaye, J., S. Penkett, and F. Ormond, *Concentrations, Lifetimes, and Trends of CFCs, Halons, and Related Species*, NASA Ref. Publ. 1339, Sci. Div. NASA Off. of Mission to Planet Earth, Washington, D. C., 1994.
- Kiehl, J. T., and B. P. Briegleb, The relative roles of sulfate aerosol and greenhouse gases in climate forcing, *Science*, *260*, 311-314, 1993.
- Ko, M. K. W., and N. D. Sze, A 2-D model calculation of atmospheric lifetimes for  $\text{N}_2\text{O}$ , CFC-11 and CFC-12, *Nature*, *297*, 317-319, 1982.
- Ko, M. K. W., N. D. Sze, and D. K. Weisenstein, Use of satellite data to constrain the model-calculated atmospheric lifetime of  $\text{N}_2\text{O}$ : Implications for other trace gases, *J. Geophys. Res.*, *96*, 7547-7552, 1991.
- Levy, H., II, J. D. Mahlman, W. J. Moxim, and S. C. Liu, Tropospheric ozone: The role of transport, *J. Geophys. Res.*, *90*, 3753-3772, 1985.
- Massie, S. T., A. Goldman, A. H. McDaniel, C. A. Cantrell, J. A. Davidson, R. E. Shetter, and J. G. Calvert, Temperature dependent infrared cross sections for CFC-11, CFC-12, CFC-13, CFC-14, CFC-22, CFC-113, CFC-114, and CFC-115, *NCAR Tech. Note NCAR/TN-358+STR*, 67 pp., Nat. Cent. for Atmos. Res., Boulder, Colo., 1991.
- McPherson, R., D., K. H. Bergman, R. E. Kistler, G. E. Rasch, and D. S. Gordon, The NMC operational global data assimilation system, *Mon. Weather Rev.*, *107*, 1445-1461, 1979.
- Meier, R. R., D. E. Anderson, and M. Nicolet, Radiation field in the troposphere and stratosphere from 240-1000 nm, I, General analysis, *Planet Space Sci.*, *30*, 923-933, 1982.
- Minschwaner, K., G. P. Anderson, L. A. Hall, and K. Yoshino, Polynomial coefficients for calculating  $\text{O}_2$  Schumann-Runge cross sections at  $0.5 \text{ cm}^{-1}$  resolution, *J. Geophys. Res.*, *97*, 10,103-10,108, 1992.
- Minschwaner, K., R. J. Salawitch, and M. B. McElroy, Absorption of solar radiation by  $\text{O}_2$ : Implications for  $\text{O}_3$  and lifetimes of  $\text{N}_2\text{O}$ ,  $\text{CFCl}_3$ , and  $\text{CF}_2\text{Cl}_2$ , *J. Geophys. Res.*, *98*, 10,543-10,561, 1993.
- Montzka, S. A., et al., Nitrous Oxide and Halocarbons Division, in *Climate Monitoring and Diagnostics Laboratory No. 20, Summary Report 1991*, edited by E. E. Ferguson and R. M. Rosson, NOAA Environ. Res. Lab., Boulder, Colo., 1992.
- Myhre, G., and F. Stordal, Role of spatial and temporal variations in the computation of radiative forcing and GWP, *J. Geophys. Res.*, *102*, 11,181-11,200, 1997.
- Oltmans, S. J., Surface ozone measurements in clean air, *J. Geophys. Res.*, *86*, 1174-1180, 1981.
- Pinnock, S., M. D. Hurley, K. P. Shine, T. J. Wallington, and T. J. Smyth, Radiative forcing of climate by hydrochlorofluorocarbons and hydrofluorocarbons, *J. Geophys. Res.*, *100*, 23,227-23,238, 1995.
- Plumb, R. A., and M. K. W. Ko, Interrelationships between mixing ratios of long-lived stratospheric constituents, *J. Geophys. Res.*, *97*, 10,145-10,156, 1992.
- Ramanathan, V., Greenhouse effect due to chlorofluorocarbons: Climatic implications, *Science*, *190*, 50-52, 1975.
- Ramanathan, V., and R. E. Dickinson, The role of stratospheric ozone in the zonal and seasonal radiative energy balance of the Earth-troposphere system, *J. Atmos. Sci.*, *36*, 1084-1104, 1979.
- Ramanathan, V., R. J. Cicerone, H. B. Singh, and J. T. Keuhl, Trace gas trends and their potential role in climate change, *J. Geophys. Res.*, *90*, 5547-5566, 1985.
- Ramanathan, V., L. Callis, R. Cess, J. Hansen, I. Isaksen, W. Kuhn, A. Lacis, F. Luther, R. Reck, and M. Schlesinger, Climate-chemical interactions and effects of changing atmospheric trace gases, *Rev. Geophys.*, *25*, 1441-1482, 1987.
- Rothman, L. S., R. R. Gamache, A. Goldman, L. R. Brown, R. A. Toth, H. M. Pickett, R. L. Poynter, J. M. Fland, C. Camy-Peyret, A. Barbe, N. Husson, C. P. Rinsland, and M. A. Smith, HITRAN database: 1986 edition, *Appl. Opt.*, *26*, 4058-4097, 1986.
- Roche, A. E., J. B. Kumer, J. L. Mergenthaler, G. A. Ely, W. G. Uplinger, J. F. Potter, T. C. James, and L. W. Sterritt, The Cryogenic Limb Array Spectrometer (CLAES) on UARS: Experiment description and performance, *J. Geophys. Res.*, *98*, 10,763-10,776, 1993.
- Rosenlof, K. H., and J. R. Holton, Estimates of the stratospheric residual circulation using the downward control principle, *J. Geophys. Res.*, *98*, 10,465-10,479, 1993.
- Rossov, W. B., and R. A. Schiffer, ISCCP cloud data products, *Bull. Am. Meteorol. Soc.*, *72*, 2-20, 1991.
- Rottman, G. J., T. N. Woods, and T. P. Sparr, Solar-Stellar Irradiance Comparison Experiment 1, 1, Instrument design and operation, *J. Geophys. Res.*, *98*, 10,667-10,678, 1993.
- Stephens, G. L., Radiation profiles in extended water clouds, I, Theory, *J. Atmos. Sci.*, *35*, 2111-2122, 1978.
- Stephens, G. L., and C. M. R. Platt, Aircraft observations of the radiative and microphysical properties of stratocumulus and cumulus cloud fields, *J. Clim. Appl. Meteorol.*, *26*, 1243-1269, 1987.
- Tans, P. P., T. J. Conway, E. J. Dlugokencky, K. W. Thoning, P. M. Lang, K. A. Masarie, P. Novelli, and L. Waterman, Carbon Cycle Division, in *Climate Monitoring and Diagnostics Laboratory No. 20, Summary Report 1991*, edited by E. E. Ferguson and R. M. Rosson, NOAA Environ. Res. Lab., Boulder, Colo., 1992.
- Volk, C. M., J. W. Elkins, D. W. Fahey, G. S. Dutton, J. M. Gilligan, M. Loewenstein, J. R. Podolske, K. R. Chan, and M. R. Gunson, Evaluation of source gas lifetimes from

- stratospheric observations, *J. Geophys. Res.*, **102**, 25,543-25,564, 1997.
- Wang, W. C., Y. L. Yung, A. A. Lacis, T. Mo, and J. E. Hansen, Greenhouse effects due to man-made perturbations of trace gases, *Science*, **194**, 685-690, 1976.
- Wang, W. C., J. P. Pinto, and Y. L. Yung, Climatic effects due to halogenated compounds in the Earth's atmosphere, *J. Atmos. Sci.*, **37**, 333-338, 1980.
- Waters, J. W., Microwave limb sounding, in *Atmospheric Remote Sensing by Microwave Radiometry*, edited by M. A. Janssen, pp. 383-496, John Wiley, New York, 1993.
- World Meteorological Organization, *Scientific Assessment of Ozone Depletion: 1991*, Global Ozone Res. and Monit. Proj., *Rep. 25*, Geneva, 1991.
- Woods, T. N., G. J. Rottman, and G. J. Ucker, Solar-Stellar Irradiance Comparison Experiment 1, 2, Instrument calibrations, *J. Geophys. Res.*, **98**, 10,679-10,694, 1993.
- Yoshino, K., A. S.-C. Cheung, J. R. Esmond, W. H. Parkinson, D. E. Freeman, and S. L. Guberman, Improved absorption cross sections of oxygen in the wavelength region 205-240 nm of the Herzberg continuum, *Planet. Space Sci.*, **36**, 1469-1475, 1988.

---

B. P. Briegleb, National Center for Atmospheric Research, Boulder, CO 80307.

R. W. Carver and K. Minschwaner, Department of Physics, New Mexico Institute of Mining and Technology, Socorro, NM 87801. (e-mail: krm@kestrel.nmt.edu)

A. E. Roche, Lockheed Palo Alto Research Laboratory, Pal Alto, CA 94304.

(Received January 19, 1998 ; revised June 2, 1998; accepted June 5, 1998.)